Triplet Exciton Confinement in Green Organic Light-Emitting Diodes Containing Luminescent Charge-Transfer Cu(I) Complexes

*Qisheng Zhang, Takeshi Komino, Shuping Huang, Shigeyuki Matsunami, Kenichi Goushi, and Chihaya Adachi**

The temperature dependence of luminescence from [Cu(dnbp)(DPEPhos)]BF_4 (dnbp = 2,9-di-n-butylphenanthroline, DPEPhos = bis[2-(diphenylphosphino) phenyl]ether) in a poly(methyl methacrylate) (PMMA) film indicates the presence of long-life green emission arising from two thermally equilibrated charge transfer (CT) excited states and one non-equilibrated triplet ligand center (^{3}LC) excited state. At room temperature, the lower triplet CT state is found to be the predominantly populated excited state, and the zero-zero energy of this state is found to be 2.72 eV from the onset of its emission at 80 K. The tunable emission maximum of [Cu(dnbp)(DPEPhos)]BF_4 in various hosts with different triplet energies is explained in terms of the multiple triplet energy levels of this complex in amorphous films. Using the high triplet energy charge transport material as a host and an exciton-blocking layer (EBL), a [Cu(dnbp)(DPEPhos)]BF_4 based organic light-emitting diode (OLED) achieves a high external quantum efficiency (EQE) of 15.0%, which is comparable to values for similar devices based on Ir(ppy)$_3$ and FIrpic. The photoluminescence (PL) and electroluminescence (EL) performance of green emissive [Cu(μI)dppb]$_2$ (dppb = 1,2-bis[diphenylphosphino]benzene) in organic semiconductor films confirmed its ^{3}CT state with a zero-zero energy of 2.76 eV as the predominant population excited state.

1. Introduction

Phosphorescent organic light-emitting diodes (PHOLEDs) containing Ir(III), Pt(III), or Os(II) based complexes generate light from both triplet and singlet excitons, allowing the internal quantum efficiency of such devices to approach 100%.[1,2] The commercial aims of the next generation of solid-state displays and light sources mean that PHOLEDs have attracted increasing attention over the last decade, although the high cost of these noble metal based phosphorescent materials is a problem. The relatively abundant, inexpensive, and non-toxic cuprous complexes appear to be an attractive alternative because their lowest triplet excited states can provide an efficient pathway for phosphorescence or reverse intersystem crossing ($T_1 \rightarrow S_1$).[3] However, apart from a few examples,[4–6] the external electroluminescence (EL) quantum efficiency (EQE) of most Cu(I) complex based OLEDs is still low (<5%),[7] despite the fact that the photoluminescence quantum yield (PLQY, φ) of green emissive Cu(I) complexes is often quite high.[7a,7c,7f,7g,7k,7m] For example, the PLQY of green-emissive [Cu(dnbp)(DPEPhos)]BF_4 (dnbp = 2,9-di-n-butylphenanthroline, DPEPhos = bis[2-(diphenylphosphino)phenyl]ether) in a poly(methyl methacrylate) (PMMA) film has been reported to be 0.69[7c] and a non-doped single layer light-emitting device using this material also achieved a high EQE of 16%,[4] which is comparable to that of the most efficient PHOLEDs.[2] However, the maximum EQE of these multilayer OLEDs with poly(vinylcarbazole) (PVK) as the host is only 3–4%.[7c] Another green emissive binuclear Cu^I complex, [Cu(μI)dppb]$_2$ (dppb = 1,2-bis[diphenylphosphino] benzene), also exhibits a PLQY as high as 0.80 in a solid state, while the maximum EQE of a device using this material with a 4,4′-bis(carbazol-9-yl)biphenyl (CBP) host and a 4,7-diphenyl-1,10-phenanthroline (BPhen) exciton-blocking layer (EBL) is only 4.8%.[7f] More recently, a codeposited CuI-mCPy (3,5-bis(carbazol-9-yl)pyridine) complex with a PLQY of 0.64 was successfully used as an emissive layer in a three-layer OLED where 2,9-dimethyl-4,7-diphenyl-1,10-phenanthroline (BCP) was used as an EBL. Bright green electroluminescence from this Cu(I) complex was observed, while the EQE of the device was still lower than 5% (EQE_{max} = 4.4%).[7m]

Recently, we found that the PLQY of [Cu(dnbp)(DPEPhos)] BF_4 and [Cu(μI)dppb]$_2$ doped in PVK (triplet energy level, T_1, = 2.5 eV) or CBP (T_1 = 2.56 eV) films is much lower than that in a

Dr. Q. Zhang, Dr. T. Komino, Dr. S. Matsunami, Dr. K. Goushi, Prof. C. Adachi
Center for Organic Photonics and Electronics Research (OPERA)
Kyushu University
744 Motooka, Nishi-ku, Fukuoka 819-0395, Japan
E-mail: Adachi@cstf.kyushu-u.ac.jp
Dr. S. Huang
Institute for Materials Chemistry and Engineering
Kyushu University
744 Motooka, Nishi-ku, Fukuoka 819-0395, Japan

DOI: 10.1002/adfm.201101907

PMMA ($T_1 \approx 3.0$ eV) film.[8] The inefficient confinement of the triplet energy on the Cu(I) complexes indicates that the triplet energy level of these green emissive Cu(I) complexes should be higher than those of CBP and PVK, which are the most commonly used host materials for green phosphorescent materials. Using high triplet energy materials as the host and the EBL, the EQE of the devices containing these two complexes were dramatically improved.[8] Here, multiple excited state energies of these two Cu(I) complexes are investigated in a solid matrix using the streak image technique. Their predominant triplet energy levels are estimated from the onset of their triplet charge-transfer (^{3}CT) emission and confirmed by comparison of their photoluminescence (PL) and EL performance levels in organic semiconductor films with those of two well-known Ir(III)-based phosphorescent materials, fac-tris(2-phenylpyridine) iridium ($Ir(ppy)_3$) and bis[(4,6-difluorophenyl)pyridinato-N,C^2](picolinato) iridium (FIrpic). Diimine Cu(I) complexes and Cu(I) halide complexes are the most extensively studied luminescent Cu(I) complexes, and $[Cu(dnbp)(DPEPhos)]BF_4$ and $[Cu(\mu I)dppb]_2$ are the first complexes found to produce efficient EL among these two types of Cu(I) complex. We believe that the studies of their triplet state energies are potentially applicable to a wide variety of Cu(I) systems.

2. Results and Discussion

The molecular structures of the emitting complexes and charge transport materials that are discussed are depicted in **Figure 1**. The photophysical properties of $[Cu(dnbp)(DPEPhos)]BF_4$ and $[Cu(\mu I)dppb]_2$ in solution or even in the solid state were thoroughly investigated by McMillin et al.[9] and Tsuboyama et al.,[7f] respectively. The lowest excited state of $[Cu(dnbp)(DPEPhos)]BF_4$ is well formulated as a charge-transfer (CT) transition involving a metal-to-ligand charge transfer (MLCT), while that of $[Cu(\mu I)dppb]_2$ can be attributed to the MLCT plus XLCT (halogen-to-ligand charge transfer), or (M+X)LCT. In the excited state, the metal cations of both complexes show divalent copper characteristics, leading to structural reorganization from tetrahedral to a square-planar geometry. Because this significant flattening distortion narrows the energy gap and increases the non-radiative decay, the photophysical properties of these two Cu(I) complexes are very sensitive to the matrix rigidity.[7c,7f] To simulate the environment in OLEDs and minimize the energy diffusion from guest to host, non-conjugated PMMA was used as the matrix for photophysical investigation of these two Cu(I) complexes and their references, $Ir(ppy)_3$ and FIrpic. All samples had the same doping concentration of 5 wt% and the same film thickness. As shown in **Figure 2**a, the PL spectra of these two Cu(I) complexes are structureless and broad, with emission maxima at 509 nm and 507 nm for $[Cu(dnbp)(DPEPhos)]BF_4$ and $[Cu(\mu I)dppb]_2$, respectively, which are blue shifted by around 40 nm from their respective spectra in a dichloromethane (DCM) solution.[7f,9,10] Although the emission maxima of these two Cu(I) complexes in PMMA films are close to the 510 nm maximum of an $Ir(ppy)_3$ doped film, the onsets of their PL spectra are blue shifted approximately 40 nm from that of $Ir(ppy)_3$ and close to that of the blue emissive FIrpic. The Stokes shifts of these two Cu(I) complexes are also much larger than those of the Ir(III) complexes. For $[Cu(dnbp)(DPEPhos)]BF_4$, the Stokes shift is as large as 130 nm between the maxima of the emission and the absorption (371 nm). In general, a structureless band and large Stokes shift are characteristics of a long-range intramolecular charge transfer (CT) parentage, such as MLCT,[11] XLCT,[3b,6,7m,12] and LLCT (ligand-to-ligand charge transfer)[13] excited states in transition metal complexes because they are more polar than their respective ground states and subsequently induce molecular structural distortion in the excited states. The characteristic flattening distortion for a MLCT Cu(I) complex magnifies the overall distortion in the excited state and results in a further red shift of the emission band.

To understand the excited state natures and measure the triplet energy levels of $[Cu(dnbp)(DPEPhos)]BF_4$ and $[Cu(\mu I)dppb]_2$ in a solid matrix, the temperature dependence of the emission spectra and the emission decay from their PMMA doped films was studied using a streak camera and the results are shown in Figure 2b,c. Using a high-power pulsed laser as the excitation source, clear time-resolved emission spectra can be obtained over a wide time range of 10 ms. The emission decay of $[Cu(dnbp)(DPEPhos)]BF_4$ in a PMMA matrix with 5 wt% concentrations can be best fitted by using three exponentials, i.e., $I = A_f\exp(-t/\tau_f)+A_m\exp(-t/\tau_m)+A_s\exp(-t/\tau_s)$, in a temperature range of 80–300 K. Lowering the temperature from 300 K to 80 K caused almost no change in the lifetime of the slow

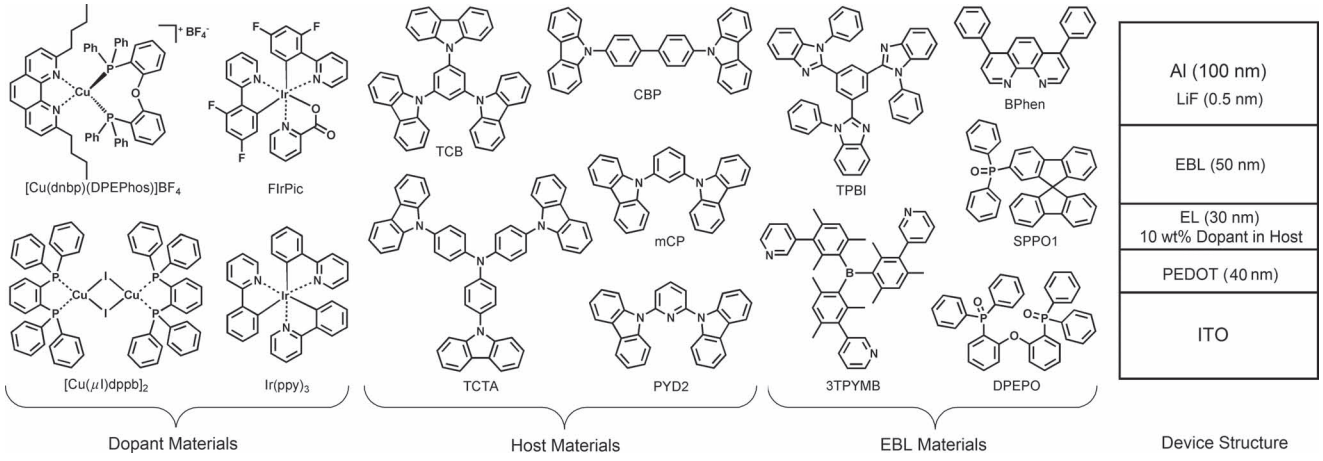

Figure 1. OLED device structure and the molecular structures of the compounds used in these devices.

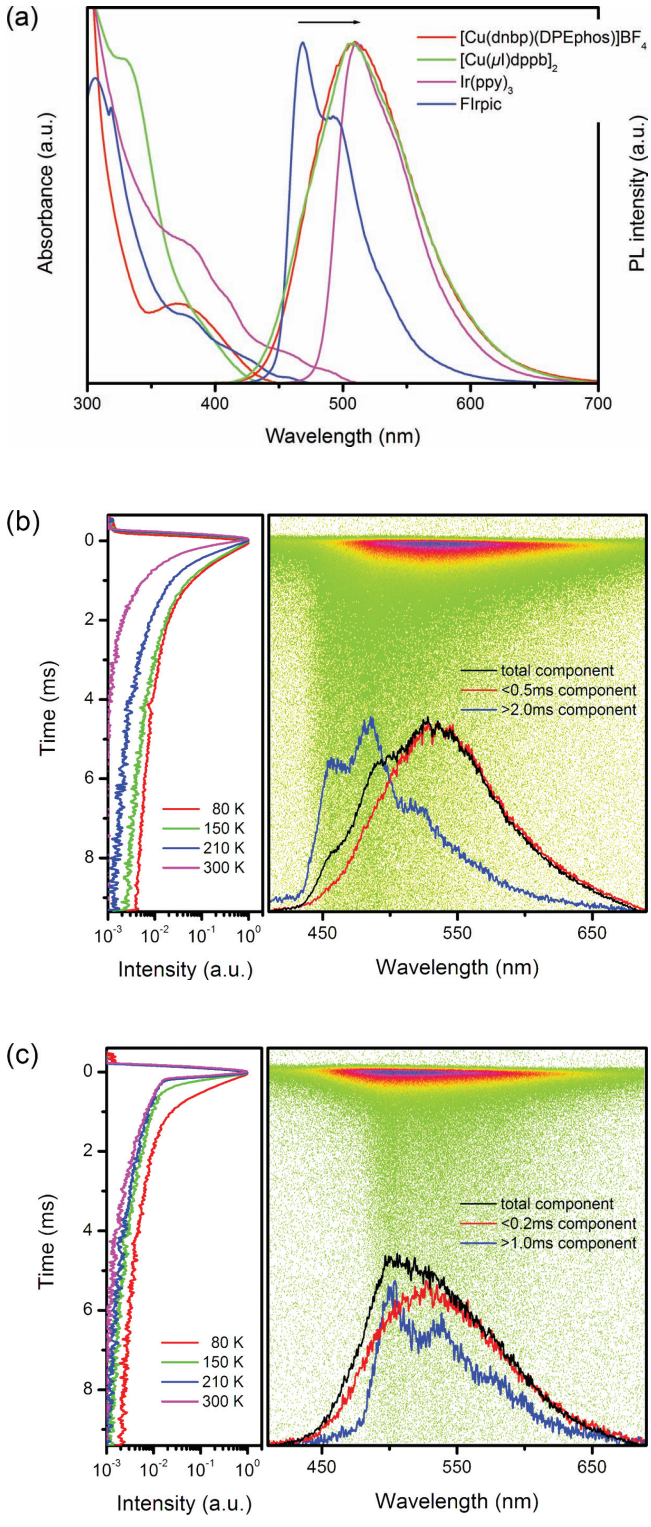

Figure 2. a) Absorption and PL spectra of 5 wt% luminescent complexes in PMMA films at room temperature. b) Streak image of a 5 wt% [Cu(dnbp)(DPEPhos)]BF_4:PMMA film at 80 K and the emission decay of the doped film at various temperatures. c) Streak image of a 5 wt% [Cu(μI)dppb]$_2$:PMMA film at 80 K and the emission decay of the doped film at various temperatures. In the streak image, the spots correspond to the intensity of PL: blue, red, yellow, and green represent very strong, strong, intermediate, and weak emissions, respectively.

component (≈7 ms), but increased its intensity. At 80 K, the long life emission band, with three distinct vibronic peaks at 455, 485, and 520 nm, can be clearly observed beside the broad CT bands, as shown in Figure 2b. In the light of the similar mixed-ligand system, $[Cu(dmp)(PPh_3)_2]^+$ (dmp = 2,9-dimethyl-1,10-phenanthroline),[14] the slow component with the vibronic emission band can be assigned to the phenanthroline ligand-centered phosphorescence (^{3}LC). However, unlike the case for a solution, the ^{3}LC phosphorescence from this mixed ligand system in a PMMA film can even be observed at room temperature (Figure S1, Supporting Information), probably because the rigid matrix limits the non-radiative decay processes caused by internal conversion. For a 5 wt% [Cu(μI)dppb]$_2$:PMMA doped film, an unexpectedly long life ^{3}LC band ($\tau_s \approx 7$ ms) with three vibronic peaks at 500, 538, and 575 nm was also observed in addition to the CT bands over the 300–80 K temperature range (Figure 2c and Figure S2, Supporting Information).

In this temperature range, the fast emission components from both the [Cu(dnbp)(DPEPhos)]BF_4 and the [Cu(μI)dppb]$_2$ doped films are the predominant components and are attributed to the CT excited states. With decreasing temperature from 300 K to 80 K, the emission maximum of the fast component red shifted from 509 nm to 533 nm for [Cu(dnbp)(DPEPhos)]BF_4 and from 507 nm to 529 nm for [Cu(μI)dppb]$_2$; the corresponding lifetimes significantly increased, from 33 μs to 263 μs for [Cu(dnbp)(DPEPhos)]BF_4 and from 6.8 μs to 210 μs for [Cu(μI)dppb]$_2$. This implies that the fast emission components of these two Cu(I) complexes may arise from two interconvertible excited states in thermal equilibrium. By applying a widely adopted two-state model built on $[Cu(dmp)_2]^+$,[15] Tsuboyama et al. demonstrated that the emission of [Cu(μI)dppb]$_2$ arises from two thermally equilibrated CT excited states, i.e., ^{1}(M+X)LCT and ^{3}(M+X)LCT. The energy difference between these two states was calculated to be approximately 0.8 eV (1.9 kcal mol^{-1}) in the solid state.[7f] For the [Cu(dnbp)(DPEPhos)]BF_4 doped film, the fast emission component at 80 K can be described as pure ^{3}CT emission because the excited state population is largely frozen in the triplet state at such a low temperature. To understand the nature of the upper CT state in equilibrium with ^{3}CT, its individual lifetime and the energy separation between it and the ^{3}CT state (ΔE) were analyzed using the two-state model. The observed lifetimes (τ_{obs}) of the fast component at various temperatures from 300 K to 80 K was examined and is summarized in **Figure 3**a. Assuming the two-state model (upper state 1 and lower state 2) is used, the observed decay rate ($k_{obs} = 1/\tau_{obs}$) can be described as a Boltzmann average using Equation (1):

$$k_{obs} = \frac{k_1 K + k_2}{1 + K} \quad (1)$$

Herein, k_1 and k_2 are the individual decay rates of states 1 and 2, respectively, $K = \frac{g_1}{g_2}\exp(-\Delta E/RT)$ and, here R, T, g_1, and g_2 denote the ideal gas constant, the absolute temperature, the degeneracies of states 1 and 2, respectively. Given the singlet character of the upper state (^{1}CT), as is commonly thought, then $g_1 = 1$ and $g_2 = 3$.[15a] An excellent fit for the kobs data in the 80–300 K temperature range was obtained with values of $k_1 = 3.8 \times 10^3$ s^{-1}, $k_2 = 4.4 \times 10^6$ s^{-1} and $\Delta E = 0.10$ eV (Figure S3, Supporting Information). This ΔE value agrees well with the energy difference between the emission maxima

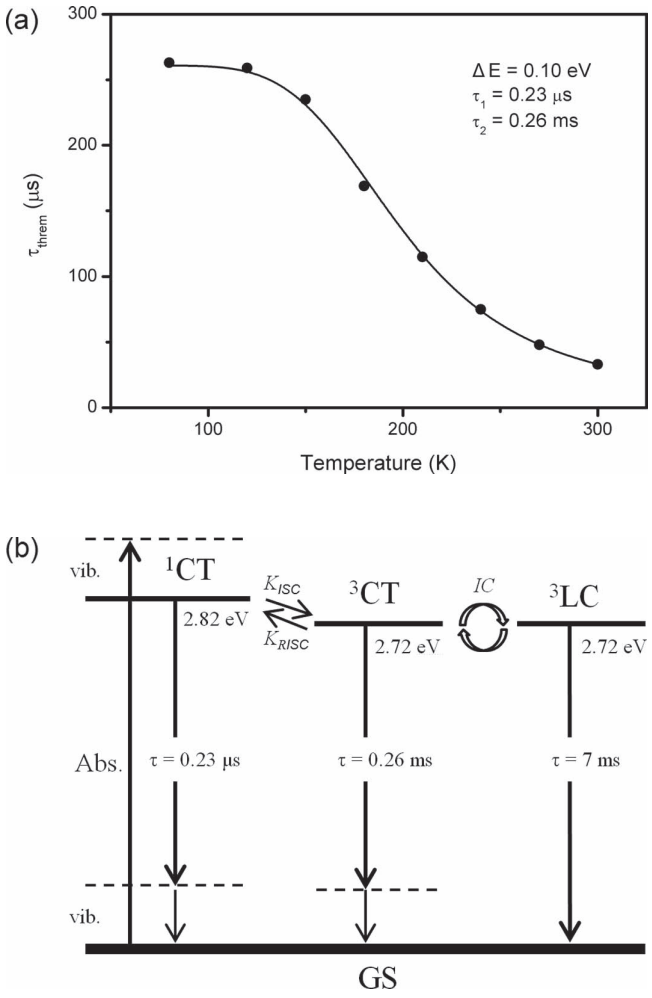

Figure 3. a) Dependence of the thermalized lifetime of [Cu(dnbp)(DPEPhos)]BF_4 in a PMMA film with 5 wt% concentration on the temperature. The solid lines were calculated using Equation 1 with parameters listed in the figure. b) The low-lying excited states for [Cu(dnbp)(DPEPhos)]BF_4 in a PMMA matrix. This three-state model can also be used to describe the photophysical properties of [Cu(μI)dppb]$_2$ in a PMMA matrix. The energy levels and individual lifetimes of the ^{1}CT, ^{3}CT, and ^{3}LC states for [Cu(μI)dppb]$_2$ are 2.84 eV, 2.76 eV, and 2.48 eV and 0.1 μs, 0.21 ms, and 7 ms, respectively.

at 80 K and 300 K (0.11 eV), indicating that the emission at room temperature results principally from the upper state by efficient up-conversion. The k_2 value corresponds to a lifetime ($\tau_2=1/k_2$) of 0.26 ms that is in accord with the experimental data for the ^{3}CT component observed at 80 K. However, the k_1 values are significantly less than those estimated for $[Cu(dmp)_2]^+$ (2×10^7 s^{-1})[15a] and [Cu(μI)dppb]$_2$ (1×10^8 s^{-1}).[7f] The corresponding lifetime (τ_1) of 0.23 μs is not typical for a fluorescence (given the triplet character for the upper state, then $g_1=g_2$ and $\tau_1=0.69$ μs), indicating that the emission of [Cu(dnbp)(DPEPhos)]BF_4 at room temperature may not only be associated with ^{1}CT, but is also contributed to by a second triplet level.[5,9] For convenience, we still designate this upper state to be ^{1}CT. Because the observed lifetime of [Cu(dnbp)(DPEPhos)]BF_4 in a PMMA film at 300 K is about two orders of magnitude higher than the isolated lifetime for the upper level, the ^{3}CT state must be the predominant population excited state between these two thermally equilibrated CT excited states at room temperature.

As described above, for a 5 wt% [Cu(dnbp)(DPEPhos)]BF_4:PMMA doped film, there is a third component with a lifetime of 0.1–0.8 ms in the 300–80 K temperature range. Because the spectrum of this middle component is very similar to that of the fast component and the values of τ_m/τ_f and A_m/A_f are almost fixed (Table S1, Supporting Information), these two components may arise from the same excited state but with different nonradiative decay processes. Therefore, a simplified three-state model can be used to describe the low lying excited states of [Cu(dnbp)(DPEPhos)]BF_4, including intersystem crossing (ISC) and reverse intersystem crossing (RISC) between ^{1}CT and ^{3}CT, and internal conversion (IC) between ^{3}CT and ^{3}LC (Figure 3b). The latter can be viewed as an intramolecular electron-transfer process ($\pi \rightarrow d$) competing with the thermalized population process (^{3}MLCT $\rightarrow$ ^{1}MLCT).[16] The zero-zero energy of the ^{3}LC state can be estimated from the highest energy vibronic component of its emission. In contrast, the zero-zero energy of a CT state must be estimated using an alternative method because its emission band is always broad and unstructured. According to the Franck–Condon principle, for fluorescent emission involving significant vibrational excitation, the zero-zero band can be roughly defined from the crossing point between absorption and emission (normalized to the same height)[17] or the average of the energies of the absorption and emission maxima.[16] Because these points are always close to the onset of the emission spectrum, the emission onset has also been used to estimate the zero-zero energy of a ^{3}MLCT state.[18] In fact, in the OLED field, the T_1 energy level of some electron-transport materials with polar groups has also been calculated from the onsets of their broad phosphorescence spectra.[19] Thus, based on the onset of the 80 K ^{3}MLCT emission band, the zero-zero energy of the ^{3}MLCT state for [Cu(dnbp)(DPEPhos)]BF_4 is estimated to be 2.72 eV in a PMMA film, which is equal to that of its ^{3}LC state (2.72 eV). This three-state model was also fitted to the [Cu(μI)dppb]$_2$ system, but the zero-zero energy of the ^{3}(M+X)LCT state (2.76 eV) is obviously higher than that of the ^{3}LC state (2.48 eV) for this complex. Although the ^{3}LC state may be the lowest triplet excited state for Cu(I) complexes, the ^{3}CT component can be the predominant state for low temperature phosphorescence due to a structurally imposed barrier against internal conversion in the rigid matrix.[16]

Time-dependent density functional theory (TD-DFT) calculations also provide some useful information for the nature of electronic excited states,[20] although the absolute value of the charge populations depends sensitively upon the choice of the basis set. Herein, the electronic ground states of [Cu(dnbp)(DPEPhos)]$^+$ were calculated based on its single-crystal structure using the DFT (B3PW91) method. As shown in **Figure 4**a, the electron density in the highest occupied molecular orbital (HOMO) is mainly associated with the Cu and P atoms, while that in the lowest unoccupied molecular orbital (LUMO) is mainly contributed by the π*-antibonding orbital of the phenanthroline ligand, suggesting a high MLCT characteristic with LLCT admixtures, i.e., (M+L)LCT.[21] The S_1 and T_1 energy levels at the ground state

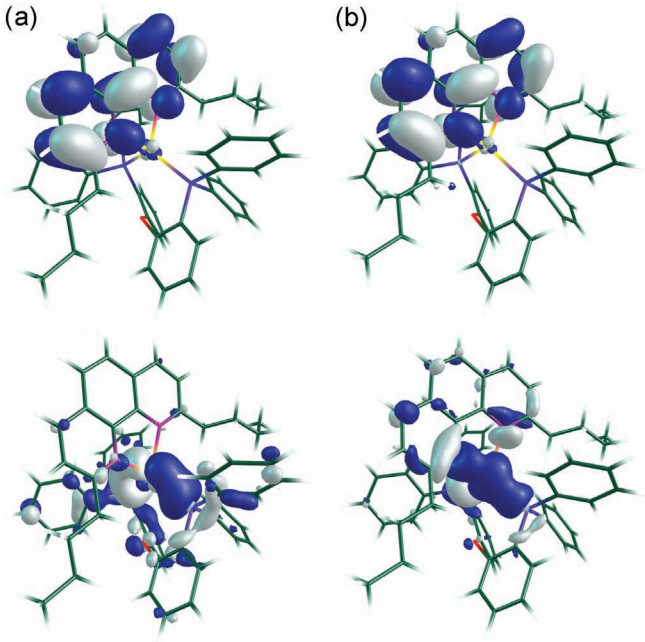

Figure 4. a) The HOMO (lower image) and LUMO (upper image) orbitals of [Cu(dnbp)(DPEPhos)]$^+$ with structures optimized in the ground state. b) The hole (lower image) and electron (upper image) distributions of [Cu(dnbp)(DPEPhos)]$^+$ with structures optimized in the lowest triplet excited state.

were calculated to be 3.02 eV and 2.74 eV, respectively, based on the TD-DFT approach. In this case, the latter is very close to the experimental data determined from a 5 wt% PMMA doped film (2.73 eV). However, the calculated energy gap between S_1 and T_1 (0.28 eV) is significantly larger than that determined from the energy difference between the emission maxima at 300 K and 80 K, which is consistent with the previous theory that the upper excited state that is thermally equilibrated with ^{3}CT is not a pure ^{1}CT state. The triplet excited states of [Cu(dnbp)(DPEPhos)]$^+$ were also calculated based on an optimized geometry of the T_1 state at the B3PW91 level. As shown in Figure 4b, the excited electron is localized on the phenanthroline ligand, while the hole resides on the Cu atom and on the phenanthroline ligand. This agrees with the deduction that the ^{3}CT and ^{3}LC states for [Cu(dnbp)(DPEPhos)]BF_4 have very similar zero-zero energy levels in the excited state. The T_1 level of this complex at its triplet excited state is found to be 1.99 eV, which is much lower than the data calculated from the ground state because the excited state geometry optimization simulates a thoroughly relaxed molecule under vacuum conditions. Although such an unresisting relaxation cannot be found under ambient conditions, it implies the seriousness of the Cu(I) → Cu(II) flattening distortion effect on the excited state energy.

As shown by the unstructured spectra and the relatively long observed lifetimes from [Cu(dnbp)(DPEPhos)]BF_4 and [Cu(μI)dppb]$_2$ at room temperature, their ^{3}CT states must be the predominant population excited states among the three low lying excited states and must play a key role in the energy transfer between guest and host. Based on the onset of their ^{3}CT emission bands, the zero-zero energy of the ^{3}CT states of these two Cu(I) complexes was estimated to be more than 2.7 eV, which is considerably higher than that of Ir(ppy)$_3$ (2.42 eV),[22] and even slightly higher than that of FIrpic (2.65 eV).[23] As a result, a high triplet energy for the host material is essential for effective triplet energy confinement on these two Cu(I) complexes, as shown by the case of FIrpic.[23,24] To determine the dependencies of their photophysical properties upon the triplet energy levels of the host materials, films of 10 wt% Cu(I) complexes in various carbazole hosts were fabricated by spin-coating. For comparison, Ir(ppy)$_3$ and FIrpic doped films were also prepared in the same way. The T_1 levels of the selected hosts, i.e., CBP, 4,4′,4″-tri(*N*-carbazolyl)triphenylamine (TCTA), 1,3,5-tri(*N*-carbazolyl)-benzene (TCB), *m*-bis(*N*-carbazolyl)benzene (mCP), and 2,6-dicarbazolo-1,5-pyridine (PYD2), were found to be 2.56,[25] 2.74,[1] 2.82,[26] 2.90,[23] and 2.93 eV,[27] respectively. As shown in **Figure 5**a, the PLQY of the doped film with a CBP host is only 0.14–0.15 for these two Cu(I) complexes. Increasing the T_1 level of the host materials gradually enhanced the PLQY of the doped films. In the PYD2 host, the PLQY values for [Cu(dnbp)(DPEPhos)]BF_4 and [Cu(μI)dppb]$_2$ are 0.56 and 0.50, respectively, and are comparable to those for a 10 wt% Ir(ppy)$_3$ doped film (0.56). It seems that the dopant with higher triplet energy is more sensitive to the triplet energy of the host. With PYD2 instead of CBP as a host, the PLQYs of the doped films based on Ir(ppy)$_3$, FIrpic, [Cu(dnbp)(DPEPhos)]BF_4, and [Cu(μI)dppb]$_2$ increase by 8%, 76%, 260%, and 260%, respectively, corresponding approximately with the order of their predominant energy levels. Herein, the PLQYs of the films doped with 10 wt% Ir(ppy)$_3$ and Firpic are note to be lower than those of the similar films fabricated by vacuum co-deposition, which are approximate 90%. In fact, a relatively low PLQY has also been found in a solution processed Ir(ppy)$_3$:CBP doped film in a previous report.[28] We suspect that more dimers with lower triplet energies may be formed in a solution-processed carbazole compound film and quench the emission from the phosphorescent complex, just as the case in a PVK film.[29] Further studies of this phenomenon are in progress.

Transient PL decay characteristics and PL spectra of 10 wt% [Cu(dnbp)(DPEPhos)]BF_4 doped in various hole transport materials are shown in Figure 5b,c. Two-component decay, i.e., a fast decay process and a slow decay process, is observed in the CBP and TCTA based films. The latter can be assigned to thermally activated triplet-triplet energy transfer between the host and the guest, which only exists in doped systems with a small triplet energy difference between guest and host, such as the FIrpic:CBP system.[23,24] However, no slow decay process was observed in a FIrpic:TCTA doped film (Figure S4, Supporting Information), indicating a lower T_1 level in FIrpic as compared to [Cu(dnbp)(DPEPhos)]BF_4. For the [Cu(dnbp)(DPEPhos)]BF_4 doped films, one unanticipated finding is a decreasing T_1 level in the host from 2.93 eV to 2.56 eV, resulting in a gradual red shift of the emission maximum from 511 nm to 535 nm, as well as a decrease in its lifetime (fast component). This phenomenon does not exist in FIrpic doped films, so it must be associated with the characteristic excited distortion of the MLCT Cu(I) complex. To explain this finding, we considered the complex microenvironment of the Cu(I) complex in organic semiconductor films and noted that the allowed distortion degree for Cu(I) complexes may be varied in these films. Consequently, in

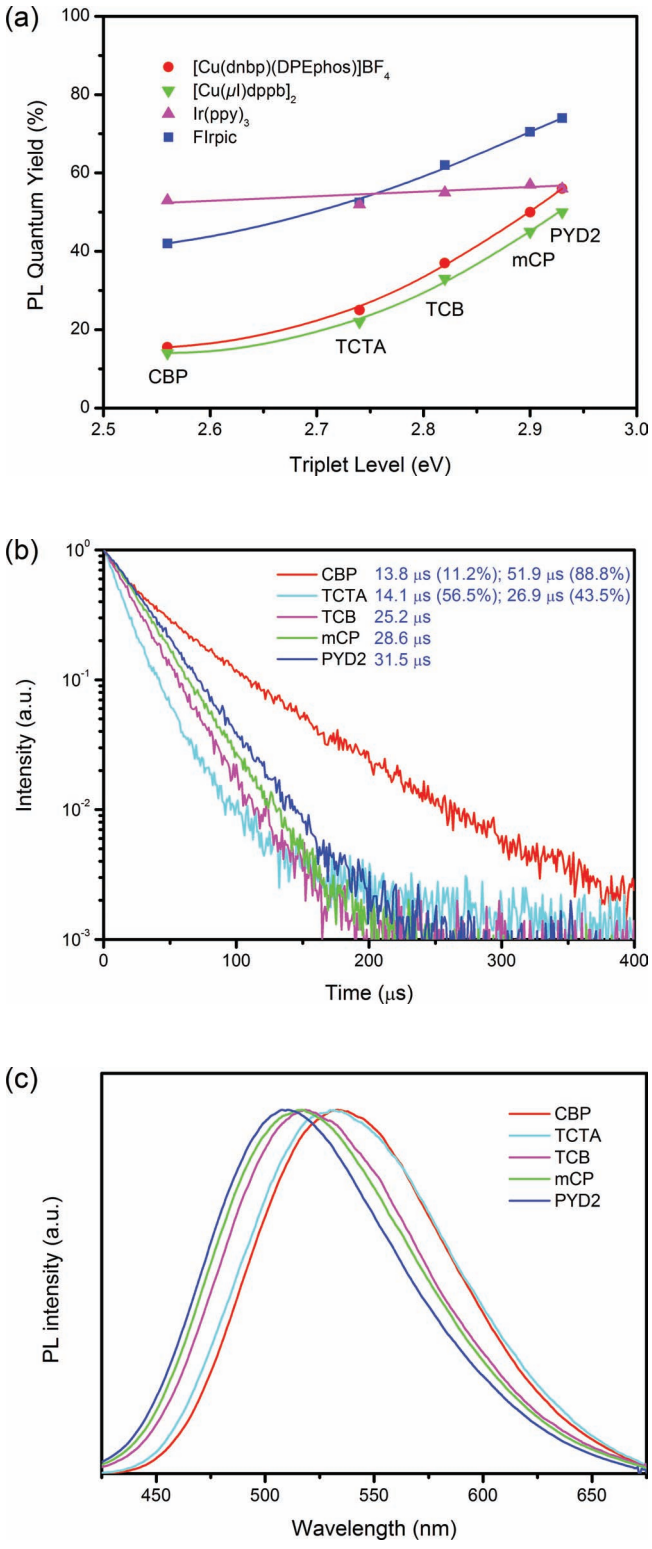

Figure 5. a) Dependence of PL quantum yield of 10 wt% luminescent complex doped films on the triplet energy level of carbazole hosts. b) Emission decay of 10 wt% [Cu(dnbp)(DPEPhos)]BF_4 doped in various host layers. c) PL spectra of 10 wt% [Cu(dnbp)(DPEPhos)]BF_4 doped in various host layers.

organic semiconductor films, the energy level of the ^{3}CT state of a Cu(I) complex is not unique, but is multi-level. During the energy transfer process, the higher triplet energy is more easily transferred from the Cu(I) complex to the host, and this effect is most noticeable when the energy gap between the triplet levels of the guest and the host is relatively small, as described above. Because the lower excitation energy corresponds to a larger non-radiative decay and a shorter lifetime due to the energy gap law, both the excitation energy and the lifetime decrease with the decreasing T_1 energy level of the host. Similar delay components and emission red shift characteristics (Figure S5 and S6, Supporting Information) were observed in a 10 wt% [Cu(μI)dppb]$_2$:CBP doped film (λ_{max} = 540 nm).

The PLQY of the emitting layer has a major influence on the efficiency of an OLED, so one might anticipate that the EQE of devices based on these two Cu(I) complexes can be greatly improved by using a high triplet energy host material, similar to the dramatic enhancement in their photoluminescence emission. For comparison, [Cu(dnbp)(DPEPhos)]BF_4 based OLEDs were fabricated using hole-transporting CBP, TCTA, TCB, mCP, or PYD2 as the host, with a structure of indium tin oxide (ITO)/poly(3,4-ethylenedioxythiophene) (PEDOT; 40 nm)/10 wt% [Cu(dnbp)(DPEPhos)]BF_4: host(30 nm)/SPPO1(50 nm)/LiF(0.5 nm)/Al (Figure 1). The emitting layers containing the Cu(I) complex and one of the small molecular hosts was generated by spin-coating on a PEDOT-treated ITO substrate with a work function of approximately –5.2 eV. Recently, Jou et al. showed that small molecules can also form homogeneous films by spin-coating and achieve very high device efficiency.[30] Above the emitting layer, a 50 nm EBL was deposited by vacuum evaporation and was then covered by the cathode. 2-(diphenylphosphoryl)spirofluorene (SPPO1) was used as a multifunctional layer for hole and exciton-blocking and electron transport because of its promising properties, including high triplet energy (2.9 eV), a deep HOMO level, and good electron mobility.[31] The thickness of each organic layer has been carefully optimized. As the results given in **Table 1** and **Figure 6** show, the maximum EQE increased steeply for devices composed of CBP, TCTA, TCB, mCP, and PYD2. The maximum EQE and maximum brightness of the device based on the PYD2 host were 8.7% and 13820 cd m^{-2}, respectively. Both are more than twice as high as the corresponding values for the device based on a CBP host. Similar devices containing [Cu(μI)dppb]$_2$ were also fabricated with CBP and PYD2 hosts. As expected, when PYD2 was used instead of CBP as the host, the maximum EQE and brightness of the device increased dramatically from 1.9% and 2000 cd m^{-2} to 4.9% and 15500 cd m^{-2}, respectively. For both Cu(I) complex based OLEDs, their emission maxima were blue shifted with PYD2 rather than CBP as the host (**Figure 7**a,b), which is consistent with the case in PL.

Recently, other evidence has indicated that the high triplet energy level of the EBL is also key for exciton confinement in the PHOLEDs, considering that the holes and electrons always recombine at the interface between electron- and hole-transport layers.[31b,32] The experimental results summarized in Table 1 and illustrated in Figure 5b also confirmed that a 10 wt% [Cu(dnbp)(DPEPhos)]BF_4:PYD2 based device using SPPO1 or tris[3-(3-pyridyl)-mesityl]borane (3TPYMB) as the EBL had a higher maximum EQE relative to devices using the

Table 1. Turn-on voltage (V_T), maximum external quantum efficiency (EQE_{max}), maximum current efficiency ($\eta_{c,max}$), maximum power efficiency ($\eta_{p,max}$), maximum brightness (B_{max}), and emission maximum (λ_{max}) of the OLEDs with different luminescent complexes, hosts, and EBLs.

Dopant	Host	EBL	V_T [V]	EQE_{max} [%]	$\eta_{c,max}$ [cd A^{-1}]	$\eta_{p,max}$ [lm W^{-1}]	B_{max} [cd m^{-2}]	λ_{max} [nm]
[Cu(dnbp)(DPEPhos)]BF_4	CBP	SPPO1	8.0	3.4	11.6	3.6	5598 (19 V)	539
	TCTA	SPPO1	6.4	3.9	13.3	5.5	2841 (18 V)	535
	TCB	SPPO1	7.1	5.4	19.9	7.0	5317 (18 V)	538
	mCP	SPPO1	6.7	6.6	21.3	8.3	10 780 (19 V)	528
	PYD2	SPPO1	6.3	8.7	28.6	12.8	13 820 (18 V)	524
	PYD2	BPhen	5.0	2.6	8.6	3.6	17 680 (13 V)	525
	PYD2	TPBI	5.3	6.3	20.5	9.9	19 940 (14 V)	520
	PYD2	3TPYMB	6.1	8.6	26.7	11.1	8980 (19 V)	511
	PYD2	DPEPO	5.6	15.0	49.5	22.3	3272 (23 V)	507
[Cu(μI)dppb]$_2$	CBP	SPPO1	7.5	1.9	6.2	2.1	2014 (19 V)	545
	PYD2	SPPO1	6.1	4.9	16.2	6.3	15 450 (19 V)	530
	PYD2	DPEPO	4.7	9.0	30.6	14.8	14 400 (23 V)	517
$Ir(ppy)_3$	PYD2	SPPO1	4.0	12.9	49.5	24.2	32 150 (18 V)	517
	PYD2	DPEPO	3.9	13.7	51.5	29.9	26 810 (22 V)	515
FIrpic	PYD2	SPPO1	6.0	14.2	32.7	14.6	19 200 (13 V)	475, 499
	PYD2	DPEPO	5.6	18.3	40.2	15.0	6262 (19 V)	475, 498

BPhen or 1,3,5-tris(*N*-phenylbenzimidazol-2-yl)benzene (TPBI) EBL. The T_1 level of 3TPYMB was reported to be higher than 2.9 eV[19a] and is comparable to that of SPPO1, while BPhen and TPBI have relatively low T_1 levels of 2.5 eV and 2.6 eV, respectively. We note that triphenylphosphine oxide (TPPO), the parent compound of SPPO1, has a high triplet energy exceeding 3.4 eV, and we find that the triplet energy of phosphine oxide based electron transport materials (ETMs) can be further raised by interrupting the direct phenyl-phenyl linkages in the molecules. The oxidation product of DPEPhos, DPEPO,[33] looks promising because of its short conjugation length and high morphological stability (Figure S7, Supporting Information). Xu et al. recently demonstrated that this high triplet energy (T_1 = 3.00 eV) dimeric triphenylphosphine oxide can be used as a host for blue PHOLEDs.[34] Herein, we found that the PLQY values of 10 wt% [Cu(dnbp)(DPEPhos)]BF_4, [Cu(μI)dppb]$_2$ and FIrpic in DPEPO films are as high as 0.59, 0.71, and 0.86, corresponding to those of 0.30, 0.41, and 0.70 in SPPO1 films, respectively. These values are also significantly higher than values for these films based on various commercially available ETMs (Table S2, Supporting Information). One may wonder why SPPO1 and 3TPYMB cannot confine the triplet exciton in doped FIrpic and Cu(I) complexes completely, given that they possess a high triplet energy of 2.9 eV. As an explanation, the ETMs with electron-withdrawing groups tend to form excimers with low triplet energies in the solid state,[35] while DPEPO can avoid such excimer formation by its special twisted structure. Since the theme of this paper is not the novel high triplet ETMs, we will report our findings in detail in another paper.

Using electron-transporting DPEPO as the EBL, devices containing 10 wt% [Cu(dnbp)(DPEPhos)]BF_4, [Cu(μI)dppb]$_2$, $Ir(ppy)_3$, or FIrpic in a PYD2 layer were fabricated and compared with the corresponding devices using a SPPO1 layer. As predicted from the photoluminescence, with DPEPO instead of SPPO1 as the EBL, the maximum EQE increased from 8.6% to 15.0% for [Cu(dnbp)(DPEPhos)]BF_4, from 4.9% to 9.1% for [Cu(μI)dppb]$_2$, and from 14.2% to 18.3% for FIrpic (see Table 1 and Figure 6b,c). The EQEs of 15.0% and 18.3% are among the best values for solution-processed electroluminescent devices based on Cu(I) complex,[4] and FIrpic,[36,37] respectively. In contrast, the maximum EQE of the $Ir(ppy)_3$ based device only increased slightly, from 12.9% to 13.7%, when a DPEPO layer was used instead of the SPPO1 layer. The rate of the maximum EQE growth seems to agree with the dependence shown in Figure 4a for the photoluminescence case. It should be noted that the optimal doping concentration for the control devices based on $Ir(ppy)_3$ and FIrpic is 10 wt% and 5 wt%, respectively. Lowering the doping concentration from 10 wt% to 5 wt% for the $Ir(ppy)_3$ based device will increase its maximum EQE slightly (Figure S8, Supporting Information). The replacement of the SPPO1 layer with a DPEPO layer also led to a further blue shift of the EL spectra of these two Cu(I) complexes, indicating that the exciton recombination region is very close to the EBL, which can be regarded as a second host for the emitter. Though the DPEPO layer improved the device efficiency by triplet exciton confinement, the current density of the DPEPO device is very low compared to that of the SPPO1 based device at the same voltage (Figure S9, Supporting Information). As reported previously, decreasing the π-conjugation of a charge transport material inevitably decreases its charge mobility.[38] In addition, the high LUMO level of DPEPO (2.0 eV for DPEPO Vs. 2.7 eV for SPPO1) also results in a high electron injection barrier between electron transport layer and cathode.

As shown in Figure 6c, with PYD2 as the host and DPEPO as the EBL, the EQE of a [Cu(μI)dppb]$_2$ based device is lower than that of an $Ir(ppy)_3$ based device, although the PLQY values of these two complexes are similar in a PYD2 film at a concentration of 10 wt%. Using a photoelectron spectroscopy (AC-2) and cooperating with its optical bandgap, the HOMO and LUMO levels of [Cu(μI)dppb]$_2$ were determined to be –5.2 eV and –2.2 eV, respectively. The former is equal to that of $Ir(ppy)_3$, while the latter is much higher than the –2.8 eV for $Ir(ppy)_3$. The ultrahigh LUMO level of [Cu(μI)dppb]$_2$ is unfavorable for electron capture in the PYD2 host, which has a similar LUMO level of –2.2 eV, leading to efficiency losses. As listed in Table 1, the turn-on voltages of [Cu(dnbp)(DPEPhos)]BF_4 and FIrpic based devices are higher than the corresponding values of $Ir(ppy)_3$ and [Cu(μI)dppb]$_2$ based devices because the HOMO levels of [Cu(dnbp)(DPEPhos)]BF_4 (–5.7 eV) and FIrpic (–5.8 eV) are comparable to those of carbazole hosts (–0.57 to –0.61 eV) and cannot afford a low barrier pathway for hole injection from the PEDOT layer to the emitting layer, as in $Ir(ppy)_3$ and [Cu(μI)dppb]$_2$. For [Cu(dnbp)

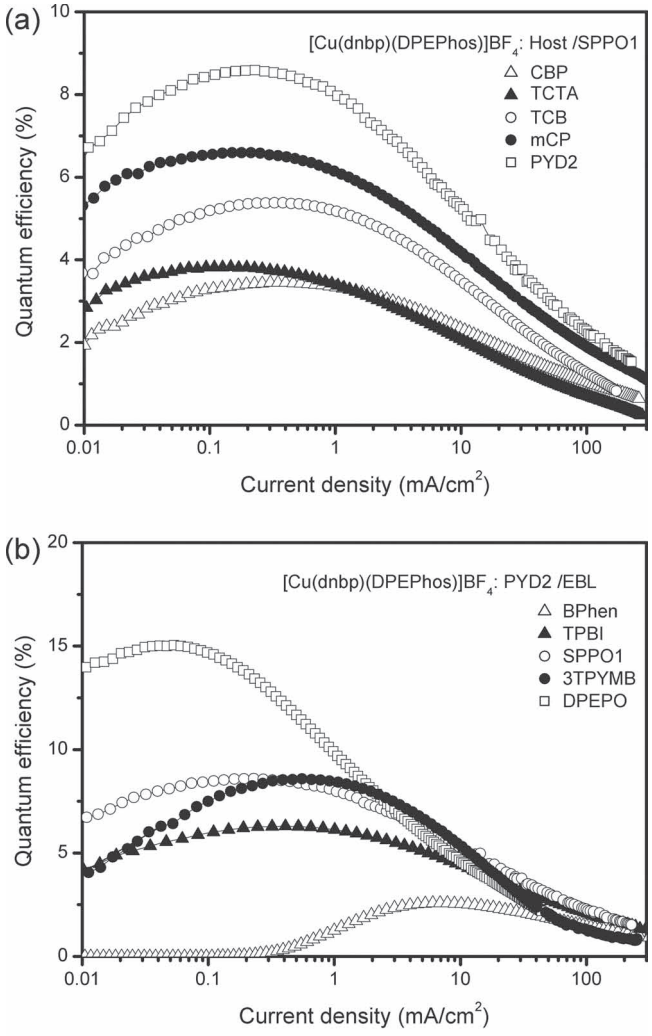

Figure 6. The EQE-current density curves of the OLEDs with different luminescent complexes, hosts, and EBLs. The general device structure is shown in Figure 1.

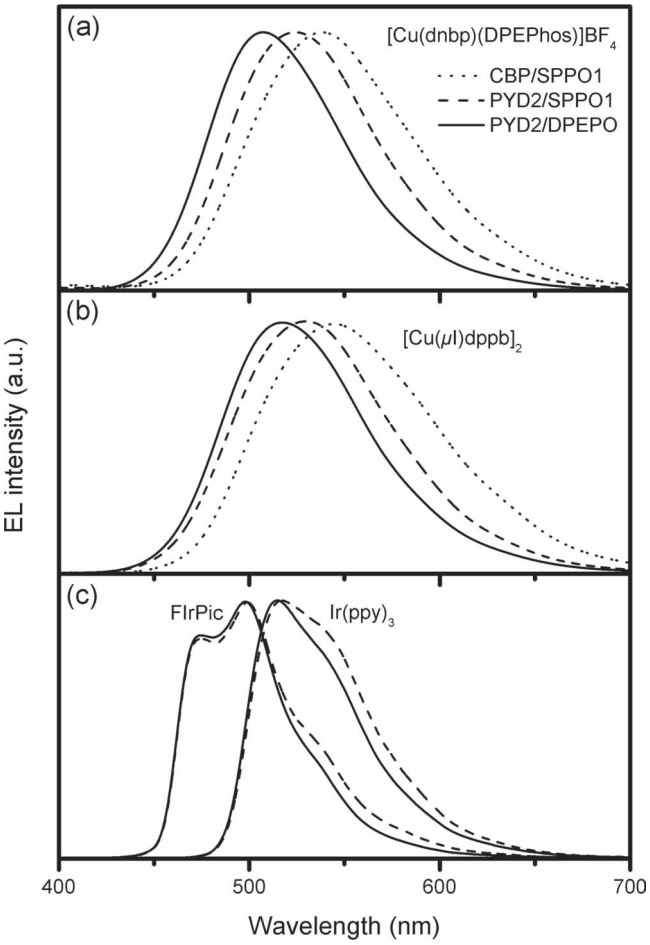

Figure 7. EL spectra of the OLEDs with different luminescent complexes, hosts, and EBLs. The general device structure is shown in Figure 1.

(DPEPhos)]BF_4 and FIrpic based devices, the large barrier between the PEDOT layer and the emitting layer (>0.5 eV) resulted in unbalanced charge injection and a low EQE at low voltage. As discussed above, using high triplet energy charge transport materials for the host and EBL means that the EL properties of these green emissive Cu(I) complexes are finally comparable with those of FIrpic, but still cannot compete with those of $Ir(ppy)_3$. The large bandgap of MLCT Cu(I) complexes limits their EL performance because of poor charge capture in the device.

3. Conclusions

Two intramolecular charge transfer Cu(I) complexes, [Cu(dnbp)(DPEPhos)]BF_4 and [Cu(μI)dppb]$_2$, have shown thermally activated emissions with broad band and large Stokes shifts. In organic semiconductor films, the PL and EL efficiencies of these Cu(I) complexes are a function of the triplet energies of the host materials. According to their PL and EL performances in various charge transport layers, the triplet energies of these green emissive Cu(I) complexes were found to be even higher than that of blue emissive FIrpic. Therefore, the triplet energy of the intramolecular charge transfer complexes cannot be simply determined from the peak of their phosphorescence spectra. Instead, the onsets of the phosphorescence spectra may lead to

a more comparable result. Although we can easily conclude that green OLEDs containing charge-transfer Cu(I) complexes can harvest both singlet and triplet excitons, and thus achieve very high EQEs (15.0%) by effective triplet exciton confinement, we must note that these Cu(I) complexes are not very favorable for OLED applications due to their ultrahigh triplet energy and large bandgap. Peters' group recently reported a type of intraligand charge transfer (ILCT) Cu(I) complexes with excited state properties that are comparable to $Ir(ppy)_3$.[5,39] However, these arylamidophosphine complexes are sensitive to oxygen and water, and their chemical stability under working conditions remains an issue.[40] Development of efficient and stable green emissive and even blue emissive Cu(I) complexes with small electronic redistribution in the excited state is a challenge for chemists. Whereas, red emitting charge-transfer Cu(I) complexes with large Stokes shifts are promising candidates for OLED applications because their relatively high triplet energy levels can decrease non-radiative decay, as predicted by the energy gap law.[41]

4. Experimental Section

Materials and Measurements: [Cu(dnbp)(DPEPhos)]BF_4, [Cu(μI)dppb]$_2$, PYD2, and DPEPO were synthesized using the following procedures described previously.[7f,9,35,42] Before device fabrication, the Cu(I) complexes were recrystallized twice from a mixture of dichloromethane/ether, while PYD2 and DPEPO were purified by sublimation after recrystallization from dichloromethane/methanol and dichloromethane/ether admixtures, respectively. PEDOT-PSS (CH8000) was purchased from H.C. Stark. $Ir(ppy)_3$, FIrpic, and other OLED materials used in this work were purchased from Luminescence Technology Corporation and used without further purification.

The samples of the luminescent complexes in the organic films were prepared by spin-coating a mixture of the complex and the organic material in dichloromethane onto a quartz glass slide. UV-vis absorption and PL spectra were recorded using a Perkin-Elmer Lambda 950-PKA UV/VIS spectrophotometer and a HORIBA Jobin-Yvon FluoroMax-4 spectrometer, respectively. The HOMO energy levels were determined by atmospheric UV photoelectron spectroscopy (Rikken Keiki AC-2). The absolute PL quantum yield was measured with an integrating sphere (C9920-02, Hamamatsu Photonics Co.) with a Xe lamp (λ_{max} = 380 nm) as the excitation source and a multichannel spectrometer (Hamamatsu PMA-11) as the optical detector. Variable temperature emission spectra and emission decay were measured using a streak camera (C4334, Hamamatsu Photonics Co.) with two different excitation sources. For measurements of the long-lived emission component (t > 1 ms), the samples were illuminated with a neodymium-doped yttrium aluminium garnet (Nd:YAG) pulsed laser (λ = 266 nm, pulse width ≈ 10 ns, repetition rate = 10 Hz). For measurements of the short-lived emission component (t < 1 ms), a N_2 gas laser (MNL200, Laser Technik Berlin, λ = 337 nm, pulse width ≈ 500 ps, repetition rate = 20 Hz) was used as the excitation source. Atomic force microscopy (AFM) images were captured using a scanning probe microscope (JEOL JSPM-5400) in tapping mode.

Quantum Chemical Calculations: TD-DFT calculations were performed using the Gaussian 09 program package.[43] The B3PW91 (Becke three-parameter exchange with Perdew–Wang-1991 correlation) functional[44] was used for both ground and excited state calculations. The LANL2DZ effective core potentials and valence basis set[45] were used to describe the valence electrons of Cu and I, with 6-31+G* applied for P and N, 6-31G* applied for C and O, and 6-31G applied for H.

Device Fabrication and Measurements: A 40 nm thick poly(3,4-ethylene dioxythiophene):poly(styrene sulfonic acid) (PEDOT:PSS) layer was spin-coated at 3000 rpm onto a pre-cleaned ITO glass substrate, followed by drying at 200°C for 10 min. Next, a 30 nm thick film of the luminescent complex and the carbazole compound was spin-coated at 1500 rpm onto the PEDOT layer from a filtered 5.5 mg mL^{-1} CH_2Cl_2 solution. After the film was dried under a vacuum for 1 h at room temperature, a 50 nm thick exciton-blocking layer was deposited in an inert chamber under a pressure of $<4 \times 10^{-4}$ Pa. Finally, the cathode was fabricated by thermal evaporation of a LiF layer (0.7 nm) followed by an Al layer (100 nm). The intersection of the ITO and the metal electrodes gives an active device area of 4 mm^2. The current density (J), voltage (V), and brightness (B) characteristics of the OLEDs were measured in ambient air with a semiconductor parameter analyzer (E5273A, Agilent) and an optical power meter (1930C, Newport). The EL spectra were recorded using a multi-channel spectrometer (UBS2000, Ocean Optics).

Supporting Information

Supporting Information is available from the Wiley Online Library or from the author.

Acknowledgements

This research was supported by the Japan Society for the Promotion of Science (JSPS) through its "Funding Program for World-Leading Innovative R&D on Science and Technology" (FIRST Program).

Received: August 14, 2011
Revised: December 27, 2011
Published online: March 19, 2012

[1] *Highly Efficient OLEDs with Phosphorescent Materials*, (Ed: H. Yersin), Wiley-VCH, Weinheim, Germany **2008**.
[2] C. Adachi, M. A. Baldo, M. E. Thompson, S. R. Forrest, *J. Appl. Phys.* **2001**, *90*, 5048.
[3] a) D. R. McMillin, K. M. Mcnett, *Chem. Rev.* **1998**, *98*, 1201; b) P. C. Ford, E. Cariati, J. Bourassa, *Chem. Rev.* **1999**, *99*, 3625; c) V. W.-W. Yam, K. K.-W. Lo, *Chem. Soc. Rev.* **1999**, *28*, 323; d) D. V. Scaltrito, D. W. Thompson, J. A. O'Callaghan, G. J. Meyer, *Coord. Chem. Rev.* **2000**, *208*, 243; e) N. Armaroli, G. Accorsi, F. Cardinali, A. Listorti, *Top. Curr. Chem.* **2007**, *280*, 69; f) A. Barbieri, G. Accorsi, N. Armaroli, *Chem. Commun.* **2008**, 2185; g) A. Lavie-Cambot, M. Cantuela, Y. Leydet, G. Jonusauskasb, D. M. Bassania, N. D. McClenaghana, *Coord. Chem. Rev.* **2008**, *252*, 2572.
[4] Q. Zhang, Q. Zhou, Y. Cheng, L. Wang, D. Ma, X. Jing, F. Wang, *Adv. Funct. Mater.* **2006**, *16*, 1203.
[5] J. C. Deaton, S. C. Switatski, D. Y. Kondakov, R. H. Young, T. D. Pawlik, D. J. Giesen, S. B. Harkins, A. J. M. Miller, S. F. Mickenberg, J. C. Peters, *J. Am. Chem. Soc.* **2010**, *132*, 9499.
[6] M. Hashimoto, S. Igawa, M. Yashima, I. Kawata, M. Hoshino, M. Osawa, *J. Am. Chem. Soc.* **2011**, *133*, 10348.
[7] a) Y. Ma, C.-M. Che, H.-Y. Chao, X. Zhou, W.-H. Chan, J. Shen, *Adv. Mater.* **1999**, *11*, 852; b) M. Noto, Y. Goto, M. Era, *Chem. Lett.* **2003**, *32*, 32; c)] Q. Zhang, Q. Zhou, Y. Cheng, L. Wang, D. Ma, X. Jing, F. Wang, *Adv. Mater.* **2004**, *16*, 432;d) W. L. Jia, T. McCormick, Y. Tao, J.-P. Lu, S. Wang, *Inorg. Chem.* **2005**, *44*, 5706; e) G. Che, Z. Su, W. Li, B. Chu, M. Li, *Appl. Phys. Lett.* **2006**, *89*, 103511; f) A. Tsuboyama, K. Kuge, M. Furugori, S. Okada, M. Hoshino, K. Ueno, *Inorg. Chem.* **2007**, *46*, 1992; g) O. Moudam, A. Kaeser, B. Delavaux-Nicot, C. Duhayon, M. Holler, G. Accorsi, N. Armaroli, I. Séguy, J. Navarro, P. Destruel, J.-F. Nierengarten, *Chem. Commun.* **2007**, 3077; h) L. Zhang, B. Li, *J. Electrochem. Soc.* **2009**, *156*, J174; i) L. Zhang, B. Li, Z. Su, *J. Phys. Chem. C* **2009**, *113*, 13968; j) D. Zhang, *J. Lumin.* **2010**, *130*, 1419; k) W. Sun, Q. Zhang, L. Qin, Y. Cheng, Z. Xie, C. Lu, L. Wang, *Eur. J. Inorg. Chem.* **2010**, 4009; l) J. Min, Q. Zhang, W. Sun, Y. Cheng, L. Wang, *Dalton Trans.* **2011**, *40*, 686; m) Z. Liu,

M. F. Qayyum, C. Wu, M. T. Whited, P. I. Djurovich, K. O. Hodgson, B. Hedman, E. I. Solomon, M. E. Thompson, *J. Am. Chem. Soc.* **2011**, *133*, 3700; n) C.-W. Hsu, C.-C. Lin, M.-W. Chung, Y. Chi, G.-H. Lee, P.-T. Chou, C.-H. Chang, P.-Y. Chen, *J. Am. Chem. Soc.* **2011**, *133*, 12085.

[8] Q. Zhang, S. Matsunami, C. Adachi, Efficient Green Cuprous-Based OLEDs Using a High Triplet Energy Host, presented at the A-COE 2010 & ASOMEP 2010, Seoul, Korea, November 3–5, 2010.

[9] a) D. G. Cuttell, S.-M. Kuang, P. E. Fanwick, D. R. McMillin, R. A. Walton, *J. Am. Chem. Soc.* **2002**, *124*, 6; b) S.-M. Kuang, D. G. Cuttell, D. R. McMillin, P. E. Fanwick, R. A. Walton, *Inorg. Chem.* **2002**, *41*, 3313.

[10] N. Armaroli, G. Accorsi, M. Holler, O. Moudam, J.-F. Nierengarten, Z. Zhou, R. T. Wegh, R. Welter, *Adv. Mater.* **2006**, *18*, 1313.

[11] a) B. Carlson, G. D. Phelan, W. Kaminsky, L. Dalton, X. Jiang, S. Liu, A. K.-Y. Jen, *J. Am. Chem. Soc.* **2002**, *124*, 14162; b) Y.-M. Cheng, G.-H. Lee, P.-T. Chou, L.-S. Chen, Y. Chi, C.-H. Yang, Y.-H. Song, S.-Y. Chang, P.-I. Shih, C.-F. Shu, *Adv. Funct. Mater.* **2008**, *18*, 183; c) H. Xia, M. Li, D. Lu, C. Zhang, W. Xie, X. Liu, B. Yang, Y. Ma, *Adv. Funct. Mater.* **2007**, *17*, 1757; d) M. Mauro, E. Q. Procopio, Y. Sun, C.-H. Chien, D. Donghi, M. Panigati, P. Mercandelli, P. Mussini, G. D'Alfonso, L. D. Cola, *Adv. Funct. Mater.* **2009**, *19*, 2607.

[12] Y.-L. Chen, S.-W. Lee, Y. Chi, K.-C. Hwang, S. B. Kumar, Y.-H. Hu, Y.-M. Cheng, P.-T. Chou, S.-M. Peng, G.-H. Lee, S.-J. Yeh, C.-T. Chen, *Inorg. Chem.* **2005**, *44*, 4287.

[13] a) H. J. Bolink, E. Coronado, R. D. Costa, N. Lardiés, E. Ortí, *Inorg. Chem.* **2008**, *47*, 9149; b) G. S. M. Tong, Y.-C. Law, S. C. F. Kui, N. Zhu, K. H. Leung, D. L. Phillips, C.-M. Che, *Chem. Eur. J.* **2010**, *16*, 6540.

[14] R. A. Rader, D. R. McMillin, M. T. Buckner, T. G. Matthews, D. J. Casadonte, R. K. Lengel, S. B. Whittaker, L. M. Darmon, F. E. Lytle, *J. Am. Chem. Soc.* **1981**, *103*, 5906.

[15] a) J. R. Kirchhoff, R. E. Gamache, M. W. Blaskie, A. A. Del Paggio, R. L. Lengel, D. R. McMillin, *Inorg. Chem.* **1983**, *22*, 2380; b) R. M. Everly, D. R. McMillin, *J. Phys. Chem.* **1991**, *95*, 9071.

[16] a) D. J. Casadonte Jr., D. R. McMillin, *J. Am. Chem. Soc.* **1987**, *109*, 331; b) D. J. Casadonte Jr., D. R. McMillin, *Inorg. Chem.* **1987**, *26*, 3950.

[17] P. Klán, J. Wirz, *Photochemistry of organic compounds: from concepts to practice*, Wiley, Chichester, UK **2009**, pp. 43.

[18] D. S. Tyson, F. N. Castellano, *J. Phys. Chem. A* **1999**, *103*, 10955.

[19] a) D. Tanaka, T. Takeda, T. Chiba, S. Watanabe, J. Kido, *Chem. Lett.* **2007**, *36*, 262; b) S.-J. Su, Y. Takahashi, T. Chiba, T. Takeda, J. Kido, *Adv. Funct. Mater.* **2009**, *19*, 1260.

[20] Marek Z. Zgierski, *J. Chem. Phys.* **2003**, *118*, 4045.

[21] a) L. Yang, J.-K. Feng, A.-M. Ren, M. Zhang, Y.-G. Ma, X.-D. Liu, *Eur. J. Inorg. Chem.* **2005**, 1867; b) T. McCormick, W.-L. Jia, S. Wang, *Inorg. Chem.* **2006**, *45*, 147; c) L. Qin, Q. Zhang, W. Sun, J. Wang, C. Lu, Y. Cheng, L. Wang, *Dalton Trans.* **2009**, *38*, 9388.

[22] K. Goushi, R. Kwong, J.J. Brown, H. Sasabe, C. Adachi, *J. Appl. Phys.* **2004**, *95*, 7798.

[23] R. J. Holmes, S. R. Forresta, Y.-J. Tung, R. C. Kwong, J. J. Brown, S. Garon, M. E. Thompson, *Appl. Phys. Lett.* **2003**, *82*, 2422.

[24] S. Tokitoa, T. Iijima, Y. Suzuri, H. Kita, T. Tsuzuki, F. Sato, *Appl. Phys. Lett.* **2003**, *83*, 569; b) Y. Kawamura, K. Goushi, J. Brooks, J. J. Brown, H. Sasabe, C. Adachi, *Appl. Phys. Lett.* **2005**, *86*, 071104.

[25] M. A. Baldo, S. R. Forrest, *Phys. Rev. B* **2000**, *62*, 10958.

[26] T. Thomsa, S. Okadab, J.-P. Chena, M. Furugori, *Thin Solid Films* **2003**, *436*, 264.

[27] K. S. Son, M. Yahiro, T. Imai, H. Yoshizaki, C. Adachi, *J. Photopolym. Sci. Technol.* **2007**, *20*, 47.

[28] W. Holzer, A. Penzkofer, T. Tsuboi, *Chem. Phys.* **2005**, *308*, 93.

[29] V. Jankus, A. P Monkman, *Adv. Funct. Mater.* **2011**, *21*, 3350.

[30] J.-H. Jou, M.-F. Hsu, W.-B. Wang, C.-L. Chin, Y.-C. Chung, C.-T. Chen, J.-J. Shyue, S.-M. Shen, M.-H. Wu, W.-C. Chang, C.-P. Liu, S.-Z. Chen, H.-Y. Chen, *Chem. Mater.* **2009**, *21*, 2565.

[31] a) S. O. Jeon, K. S. Yook, C. W. Joo, J. Y. Lee, *Opt. Lett.* **2009**, *34*, 407; b) S. O. Jeon, K. S. Yook, C. W. Joo, J. Y. Lee, *Appl. Phys. Lett.* **2009**, *94*, 013301; c) S. O. Jeon, K. S. Yook, C. W. Joo, H. S. Son, J. Y. Lee, *Thin Solid Films* **2010**, *518*, 3716.

[32] a) N. Chopra, J. Lee, Y. Zheng, S.-H. Eom, J. Xue, F. Soa, *Appl. Phys. Lett.* **2008**, *93*, 143307; b) H. Sasabe, E. Gonmori, T. Chiba, Y.-J. Li, D. Tanaka, S.-J. Su, T. Takeda, Y.-J. Pu, K.-i. Nakayama, J. Kido, *Chem. Mater.* **2008**, *20*, 5951; c) S. O. Jeon, S. E. Jang, H. S. Son, J. Y. Lee, *Adv. Mater.* **2011**, *23*, 1436.

[33] a) J. Fawcett, A. W. G. Platt, S. Vickers, M. D. Ward, *Polyhedron* **2004**, *23*, 2561; b) S. Biju, M. L. P. Reddy, A. H. Cowley, K. V. Vasudevan, *Cryst. Growth Des.* **2009**, *9*, 3562.

[34] C. Han, Y. Zhao, H. Xu, J. Chen, Z. Deng, D. Ma, Q. Li, P. Yan, *Chem. Eur. J.* **2011**, *17*, 5800.

[35] P. A. Vecchi, A. B. Padmaperuma, H. Qiao, L. S. Sapochak, P. E. Burrows, *Org. Lett.* **2006**, *8*, 4211.

[36] a) W. Jiang, L. Duan, J. Qiao, D. Zhang, G. Dong, L. Wang, Y. Qiu, *J. Mater. Chem.* **2010**, *20*, 6131; b) W. Jiang, L. Duan, J. Qiao, G. Dong, L. Wang, Y. Qiu, *Org. Lett.* **2011**, *13*, 3146.

[37] a) J. Ding, B. Zhang, J. Lü, Z. Xie, L. Wang, X. Jing, F. Wang, *Adv. Mater.* **2009**, *21*, 4983; b) S. Ye, Y. Liu, J. Chen, K. Lu, W. Wu, C. Du, Y. Liu, T. Wu, Z. Shuai, G. Yu, *Adv. Mater.* **2010**, *22*, 4167; c) J.-H. Jou, W.-B. Wang, S.-Z. Chen, J.-J. Shyue, M.-F. Hsu, C.-W. Lin, S.-M. Shen, C.-J. Wang, C.-P. Liu, C.-T. Chen, M.-F. Wu, S.-W. Liu, *J. Mater. Chem.* **2010**, *20*, 8411.

[38] a) V. Getautis, O. Paliulis, V. Gaidelis, V. Jankauskas, J. Sidaravičius, *J. Photochem. Photobiol. A: Chem.* **2002**, *151*, 39; b) B.-C. Wanga, H.-R. Liaoa, J.-C. Changb, L. Chenb, J.-T. Yeh, *J. Lumin.* **2007**, *124*, 333.

[39] a) S. B. Harkins, J. C. Peters, *J. Am. Chem. Soc.* **2005**, *127*, 2030; b) A. J. M. Miller, J. L. Dempsey, J. C. Peters, *Inorg. Chem.* **2007**, *46*, 7244.

[40] K. J. Lotito, J. C. Peters, *Chem. Comm.* **2010**, *46*, 3690.

[41] a) Q. Zhang, Q. Zhou, Y. Cheng, L. Wang, D. Ma, X. Jing, F. Wang, *Chin. J. Appl. Chem.* **2006**, *23*, 570; b) Q. Zhang, Y. Cheng, L. Wang, Z. Xie, X. Jing, F. Wang, *Adv. Funct. Mater.* **2007**, *17*, 2983.

[42] E. L. Williams, K. Haavisto, J. Li, G. E. Jabbour, *Adv. Mater.* **2007**, *19*, 197.

[43] Gaussian 09, Revision A.02, M. J. Frisch, G. W. Trucks, H. B. Schlegel, G. E. Scuseria, M. A. Robb, J. R. Cheeseman, G. Scalmani, V. Barone, B. Mennucci, G. A. Petersson, H. Nakatsuji, M. Caricato, X. Li, H. P. Hratchian, A. F. Izmaylov, J. Bloino, G. Zheng, J. L. Sonnenberg, M. Hada, M. Ehara, K. Toyota, R. Fukuda, J. Hasegawa, M. Ishida, T. Nakajima, Y. Honda, O. Kitao, H. Nakai, T. Vreven, H. A. Montgomery Jr., J. E. Peralta, F. Ogliaro, M. Bearpark, J. J. Heyd, E. Brothers, K. N. Kudin, V. N. Staroverov, R. Kobayashi, J. Normand, K. Raghavachari, A. Rendell, J. C. Burant, S. S. Iyengar, Tomasi, M. Cossi, N. Rega, J. M. Millam, M. Klene, J. E. Knox, J. B. Cross, V. Bakken, J. C. Adamo, J. Jaramillo, R. Gomperts, R. E. Stratmann, O. Yazyev, A. J. Austin, R. Cammi, C. Pomelli, J. W. Ochterski, R. L. Martin, K. Morokuma, V. G. Zakrzewski, G. A. Voth, P. Salvador, J. J. Dannenberg, S. Dapprich, A. D. Daniels, O. Farkas, J. B. Foresman, J. V. Ortiz, J. Cioslowski, D. J. Fox, Gaussian, Inc., Wallingford, CT **2009**.

[44] a) A. D. Becke, *J. Chem. Phys.* **1993**, *98*, 5648; b) J. P. Perdew, in *Electronic Structure of Solids*, (Eds: P. Ziesche, H. Eschrig), Akademie Verlag, Berlin, Germany **1991**, pp. 11–20; c)J. P. Perdew, J. A. Chevary, S. H. Vosko, K. A. Jackson, M. R. Pederson, D. J. Singh, C. Fiolhais, *Phys. Rev. B* **1992**, *46*, 6671; d) J. P. Perdew, Y. Wang, *Phys. Rev. B* **1992**, *45*, 13244.

[45] P. J. Hay, W. R. Wadt, *J. Chem. Phys.* **1985**, *82*, 270.